ChemInform Abstract: Oxidation of Cesium-Modified Graphite Supported on a Ru(001) Surface.

ARTICLE *in* CHEMINFORM · AUGUST 2010

Impact Factor: 0.74 · DOI: 10.1021/j100010a038

2 AUTHORS:

Yaw-Wen Yang
National Synchrotron Radiation Research Ce…
120 PUBLICATIONS **1,156** CITATIONS
SEE PROFILE

Jan Hrbek
Brookhaven National Laboratory
214 PUBLICATIONS **6,039** CITATIONS
SEE PROFILE

Oxidation of Cesium-Modified Graphite Supported on a Ru(001) Surface

Y. W. Yang[†] and J. Hrbek*

Chemistry Department 555, Brookhaven National Laboratory, Upton, New York 11973-5000

Received: June 22, 1994; In Final Form: September 30, 1994[⊗]

The oxidation of Cs-modified graphite supported on a Ru(001) surface has been investigated by thermal desorption spectroscopy (TDS) and X-ray photoelectron spectroscopy (XPS). The major oxidation products are CO and CO_2 with a product ratio of about 2:1; in contrast, for the nonmodified case, the oxidation of graphite leads only to the formation of CO. XPS results of oxygen adsorbed on a cesium-covered graphitic surface indicate the presence of Cs peroxide and Cs superoxide with Cs peroxide being the most thermally stable species. Oxygen released from Cs peroxide decomposition at elevated temperature enhances the oxidation of graphite and leads to an unusually narrow CO desorption feature, while the graphite oxidation in the absence of Cs is characterized by a broad CO desorption feature. The experiments demonstrate that Cs modification leads to both activity and selectivity changes in the oxidation of surface graphite. We observe a faster carbon removal and also the new reaction pathway: CO_2 formation.

I. Introduction

The oxidation of graphite has been studied extensively because of the technological relevance of this reaction in carbon gasification reactions for energy conversion. Alkali metal salts and transition metal oxides are used in these reactions as effective catalysts. An overview of the subject and results of a model study exploring the modification of graphite gasification by potassium metal can be found in recent work.[1]

The reactions of surface carbon adsorbed on transition metal surfaces are also of great interest for their relevance to the activity of metal catalysts, e.g. in methanation and Fisher−Tropsch synthesis. From the reactivity studies of carbonaceous species on metal single crystals[2,3] and on real catalysts,[4] it was suggested that two types of carbon exist on the surfaces. These two carbon species have distinct signatures in both Auger and XPS spectra: active carbon resembles metal carbides, whereas inactive carbon is similar to graphite. The transformation of carbidic into graphitic carbon occurs through an annealing to high temperature. It is believed that the formation of graphite is responsible for the poisoning (coking) of industrial catalysts; therefore, it is important to investigate the removal of graphite from metal surfaces.

There have been only few studies of graphite oxidation on metal surfaces.[5−8] In general, graphite is chemically inert, and oxygen does not chemisorb on graphite. Sau and Hudson[5] studied the oxidation of a graphite monolayer on Ni(110) and observed that the rate-limiting step was the initial adsorption of oxygen at the defects of the graphite layer, i.e. on the bare metal surface not covered by graphite. Schafer and Wassmuth[6] studied the oxidation of graphite on Pt(111) and suggested that the product formation rate is limited by the amount of oxygen sticking to the metal surface. These studies point to an important factor in achieving a complete oxidative removal of surface graphite: the presence of coadsorbed oxygen on metal substrates is crucial as graphite does not adsorb oxygen.

The coadsorption of alkali metals with simple molecules on metal surfaces is a very active area of surface research.[9] Alkali metals are reactive toward oxygen and form oxides of varying stoichiometry ranging from suboxide, oxide, peroxide, to superoxide.[10] Through the oxide formation, alkali metals can retain large amounts of relatively weakly bound and reactive oxygen. This notable feature is exploited in the present work to facilitate a complete removal of graphite from the surface.

We report a cesium-modified oxidation of graphite studied by TDS and XPS. We find that Cs alters and enhances the graphite oxidation by retaining large amounts of oxygen on top of the graphite overlayer. These oxygen species are present in the form of peroxide at elevated temperature, as compared to atomic oxygen in the nonmodified case. This change of the oxygen entity leads to the different oxidation chemistry.

II. Experimental Section

Experiments were performed in two ion-pumped ultrahigh-vacuum (UHV) chambers with two separate Ru(001) crystals at a chamber base pressure better than 2×10^{-10} Torr. The first chamber was equipped with AES, LEED, a sputter gun, and a differentially pumped quadrupole mass spectrometer. The second chamber contained a mass spectrometer, a sputter gun, an X-ray source, and a hemispherical energy analyzer for XPS measurements. XPS spectra were obtained with the Mg Kα line. The details of crystal mounting and cleaning were described earlier.[11] Cesium metal was dispensed from a commercial SAES getter. During Cs evaporation the chamber pressure rose to less than 5×10^{-10} Torr.

The graphite layer was formed by the thermal decomposition of either an ethylene or toluene overlayer on the Ru surface.[12−15] A repeated adsorption and decomposition of toluene (ethylene) was required to prepare high coverages of graphite on Ru. The graphite coverages were estimated by back-titrating empty Ru sites with CO adsorbate. Ethylene (Matheson Gas Products, chemical pure grade) was used without further purification, and toluene (Aldrich Chemical, HPLC grade) was purified by several cycles of freezing and thawing.

Ethylene (toluene) was adsorbed on the clean Ru(001) at room temperature. The crystal temperature was subsequently raised to 1250 K at a rate of 5 K/s and was held at the final temperature for 1 min for annealing. Thermal decomposition, as monitored by hydrogen evolution, was completed by 800 K for both precursor molecules. Hydrogen TDS spectra for both ethylene and toluene precursors are characterized by a series of closely spaced peaks that relate to the different stages of the dehydro-

[†] Permanent address: Synchrotron Radiation Research Center, Hsinchu, Taiwan 30077.

[⊗] Abstract published in *Advance ACS Abstracts*, February 15, 1995.

0022-3654/95/2099-3229$09.00/0

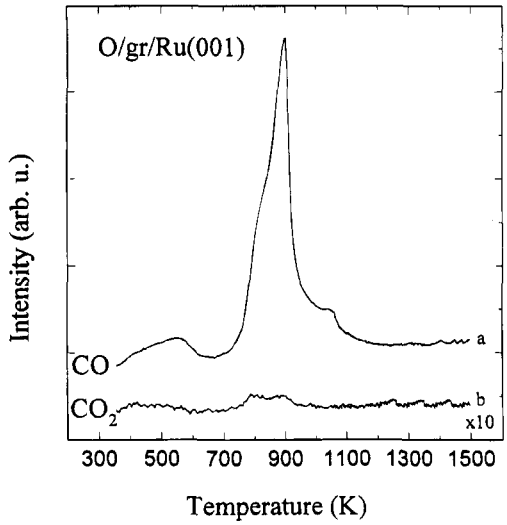

Figure 1. Oxidation of a graphite layer with products CO (a) and CO_2 (b) monitored. Graphite coverage was 0.5 ML, oxygen exposure was 6 L, and a heating rate $\beta = 5$ K/s was used.

genation reaction, and both spectra agree well with previously published data.[13-15] The formation of graphite was evidenced by an emergence of a hexagonal (9 × 9) LEED pattern. This (9 × 9) pattern was originally interpreted by a coincidence lattice formed by a nearly perfect lattice match between nine Ru and 10 graphite unit meshes along Ru close-packed direction.[16] A recent reinterpretation of the (9 × 9) pattern as an (11 × 11) structure was based on the LEED results and the STM images.[17] The formation of graphite is a general phenomenon and has been observed with LEED on many transition metal surfaces such as Ir,[18] Ni,[19] and Fe,[20] and images of graphite islands on a Pt(111) surface by STM have been reported.[21]

The coverages are reported with respect to the number of surface atoms in a closed-packed Ru(001) plane. The graphite coverages were measured by CO adsorption. A fraction of the Ru surface not covered by graphite is a ratio of the CO desorption areas from the graphite-covered Ru and from the clean Ru surface. The Cs and CO coverages were measured from TDS. A graphite monolayer (ML) has 3.8×10^{15} C atoms/cm^2 or 2.4 times the packing density of Ru(001). For a Cs ML, the packing density is one-third that of Ru(001) because the Cs monolayer has a $(\sqrt{3} \times \sqrt{3})$-R30° structure.[22]

III. Results

To simplify the bookkeeping of the adsorption sequence, a shorthand notation will be used throughout this paper. For example, a symbol of Cs/O/Ru means that oxygen is adsorbed on Ru first and the surface is dosed with the Cs metal afterward.

Thermal Desorption. ***(A) O/graphite/Ru.*** Figure 1 shows TDS of oxidation products CO and CO_2 formed during the reaction of a graphitic layer (graphite coverage was 0.5 ML) with coadsorbed oxygen. CO is the major product, and CO_2 is only formed in a small quantity at 800 K. The main CO peak at 900 K is attributed to the graphite oxidation, and the peak temperature is in good agreement with the data published earlier.[15] The small, broad peak at about 560 K is from the oxidation of surface carbon and has been discussed in detail before.[23] Note that, for a high-coverage graphite layer, a complete oxidation cannot be attained because oxygen does not stick on a graphitic surface and the number of Ru sites for oxygen adsorption is limited. As a high-coverage graphitic layer (0.9 ML) was exposed up to 40 L of oxygen, neither CO nor

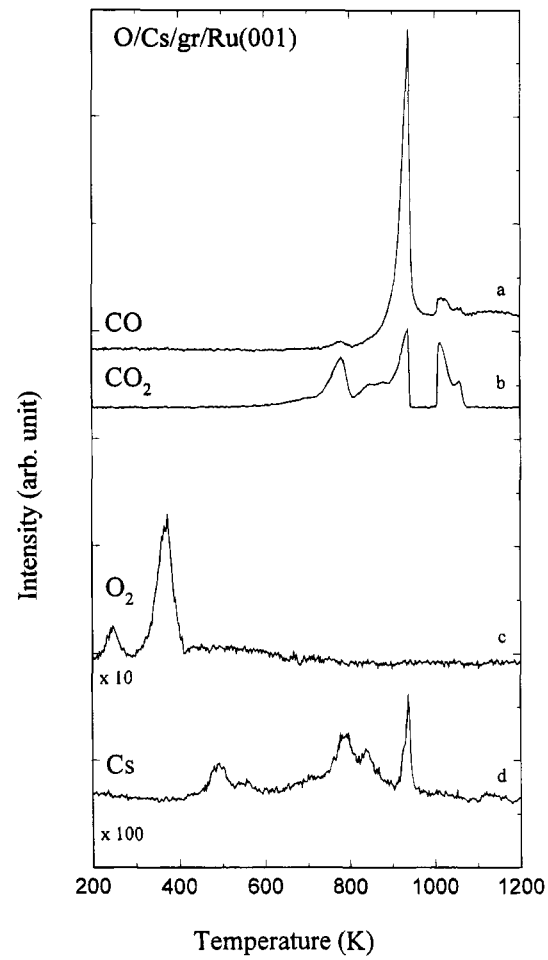

Figure 2. Cesium-modified oxidation of graphite grown on a Ru(001) surface. Four different masses were monitored simultaneously: CO (a), CO_2 (b), O_2 (c), and Cs (d). Graphite coverage was about 0.9 ML. Both Cs and oxygen adsorption were done at 200 K. $\theta_{Cs} = 1.5$ ML, oxygen exposure was 27 L, and $\beta = 2$ K/s.

CO_2 could be detected in the TDS. Moreover, no XPS O 1s signal could be detected on an oxygen-exposed graphite surface. This observation is consistent with the previous results that oxygen does not chemisorb on a graphite surface.[5,6] To remove graphite completely, several adsorption−desorption cycles are necessary.

(B) O/Cs/gRaphite/Ru. The oxidation of graphite modified by cesium is illustrated in Figure 2. The surface was prepared by forming the graphite layer first and then adsorbing Cs and oxygen sequentially. The oxidation of graphite proceeds to a full completion in one adsorption−desorption cycle, and a large amount of CO_2 is formed. The relative yields of CO to CO_2 are obtained by integrating respective peak areas, and their ratio is ~2:1.

For CO desorption, a sharp, intense peak appears at 940 K. This peak exhibits a narrow width of 20 K, which is quite unusual for a desorption occurring at such a high temperature. Besides the main peak, the other small CO features also correlate with CO_2 desorption. CO_2 desorption is noted for a series of jagged peaks, and the sudden disappearance of the desorption signal between 940 and 1010 K is intriguing. This phenomenon is reproducible. Coinciding with this CO_2 disappearance is a sudden drop in the CO desorption signal.

At the same temperature of the major CO desorption peak, an equally narrow cesium desorption peak is also observed (curve d in Figure 2). Moreover, the broad envelope of Cs desorption, starting at a temperature of 750 K, also seems to

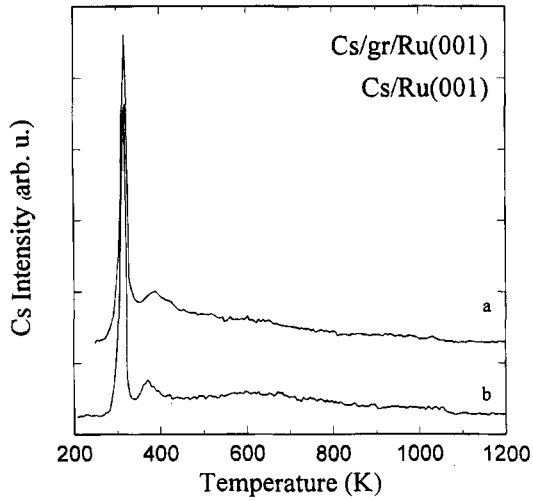

Figure 3. Cs desorption from (a) graphite-covered Ru(001) and (b) a clean Ru surface. Cs was adsorbed at 200 K. Graphite coverage was about 0.9 ML. θ_{Cs} = 1.5 ML. and β = 5 K/s.

follow the CO_2 desorption feature. This temperature correlation points to the important role played by Cs in the enhanced oxidation.

Further investigation of the oxidation will be carried out by examining systems with fewer components, and then we will proceed with added complexity. This methodology is called for because of the complicated interactions that may exist in this multicomponent system. It is known that cesium not only forms a Cs−O complex with the adsorbed oxygen[24] but also can form well-known Cs graphite intercalation compounds.[25,26] The question of which process is more important can only be addressed by the above strategy.

(C) Cs/Graphite/Ru and O/Graphite/Ru. Figure 3a shows the TDS of Cs desorbing from a 0.9 ML graphite. Also shown for comparison (Figure 3b) is the same amount of Cs (1.5 ML) desorbing from the clean Ru surface. A high-coverage graphite layer was purposely chosen to ensure that the majority of Cs atoms is adsorbed on graphite and that the contribution from Ru-bound Cs is small. For both curves, TDS of the first Cs ML desorbing from Ru(001) is characterized by a broad, featureless structure extending from 1050 K down to 320 K. Below 320 K, a sharp desorption peak that relates to the second layer can be observed.[22] The similarity between the two spectra suggests that the morhology and bonding of Cs on the graphite surface and on the clean Ru surface are comparable.

(D) O/Cs/Ru and Cs/O/Ru. The TD spectra of oxygen adsorbed on cesium layers have been reported before;[27] nevertheless, it is beneficial to examine how Cs adsorbs on an oxygen-covered surface to discern the relative strength of interactions among Cs, O, and Ru. Figure 4 shows the simultaneous desorption of oxygen and cesium from Cs/O/Ru (A) and O/Cs/Ru (B) systems. Also shown for comparison is the respective desorption of cesium and oxygen from the clean Ru surface (A).

For the O/Cs/Ru system (Figure 4B), new prominent features for both Cs and O_2 desorption are observed. The broad feature of Cs desorbing from clean Ru(001) is replaced by an intense, relatively sharp peak at 880 K. This shift toward higher temperature indicates the thermal stabilization of Cs by coadsorbed oxygen. At the same temperature, a small oxygen desorption peak is also detected, suggesting the decomposition of a Cs−O surface complex. The intensity of this peak increases with increasing θ_{Cs}. In agreement with previous work,[27] we also observed an increase of oxygen uptake on the Ru surface.

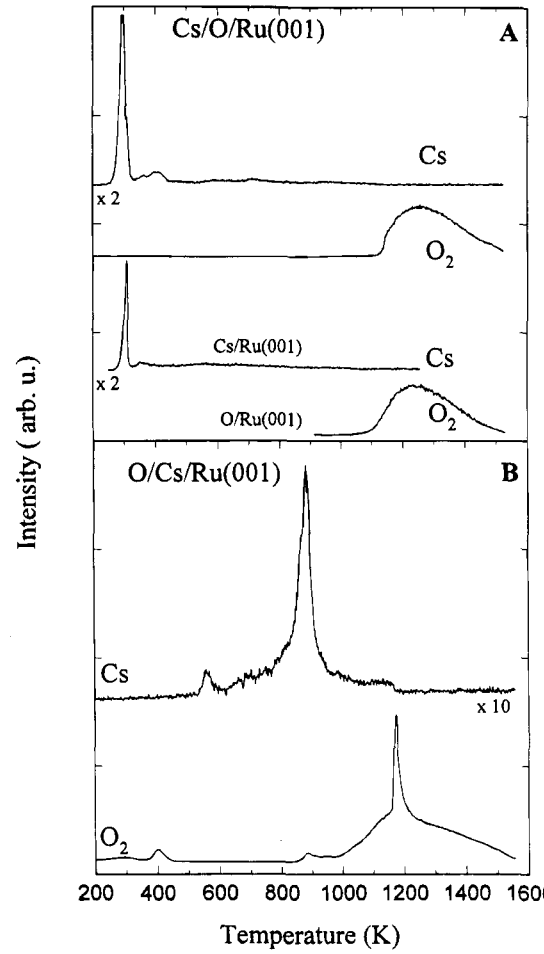

Figure 4. Thermal desorption spectra of oxygen and cesium from (A) Cs/O/Ru and (B) O/Cs/Ru. Also shown in A are oxygen from clean Ru and Cs from clean Ru. Oxygen exposures were 18 L, and cesium was adsorbed at 200 K. θ_{Cs} = 1.5 ML for Cs/Ru and O/Cs/Ru and >3 ML for Cs/O/Ru. β = 2 K/s.

It is worth mentioning the other oxygen desorption features. The sharp peak (1170 K) riding on top of the broad oxygen desorption can be traced to the codesorption of Cs with residual gases such as CO, CO_2, and H_2O. The oxygen desorption peak at 380 K relates to the decomposition of Cs superoxide, and the evidence is to be presented in the XPS section.

For Cs/O/Ru (Figure 4A), both Cs and O_2 desorb in similar fashion as though they were from a clean Ru surface. This observation suggests that Cs is not able to compete with Ru for chemisorbed oxygen to form a Cs−O complex. In view of the strong Ru−O bonding (the onset of O_2 desorption occurring at temperatures higher than 1050 K), this observation is not too surprising. However, Cs still wets the oxygenated Ru surface, and layer growth ensues as evidenced by the emergence of Cs peaks desorbing from the second and third layers.

XPS Data. Both $3d_{5/2}$ and $3d_{3/2}$ peaks of the Ru substrate show little change as overlayers are grown successively on top of it. As graphite forms on top of the Ru substrate, a shoulder on the high binding energy side of the Ru $3d_{3/2}$ peak develops due to the overlap of the Ru $3d_{3/2}$ and C 1s peaks. The observed binding energies of Ru $3d_{3/2}$ and graphite C 1s agree with the previously determined values of 285.6 and 284.1 eV.[14] As cesium and oxygen adsorb sequentially onto graphite, the intensities of Ru $3d_{5/2}$ peaks attenuate, but neither peak positions nor peak widths show any change.

Figure 5 shows Cs 3d XPS spectra obtained after adsorption of 1.8 ML of Cs on (a) Ru, (b) graphite-covered Ru, (c) (2 ×

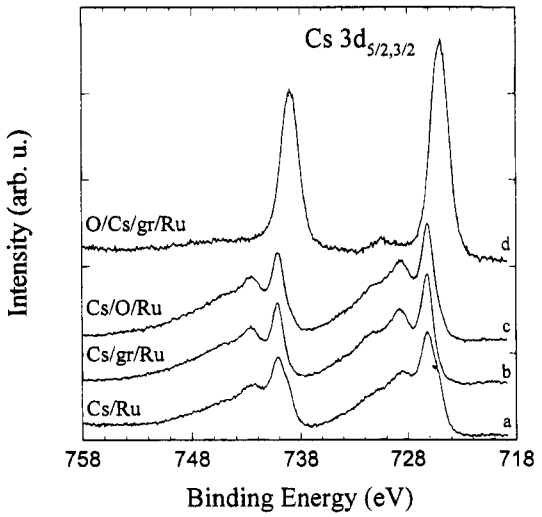

Figure 5. Cs 3d XPS spectra of Cs adsorbed on (a) clean Ru(001), (b) Cs/graphite/Ru, (c) Cs/(2 × 2)-O/Ru(001), and (d) O/Cs/graphite/Ru. Graphite coverage was estimated as about 0.9 ML, $\theta_{Cs} = 1.8$ ML, and the oxygen exposure in (d) was 27 L. Both Cs and oxygen were adsorbed at 200 K, and spectra were taken at 85 K with photoelectrons collected at an exit angle of 70° off the surface normal.

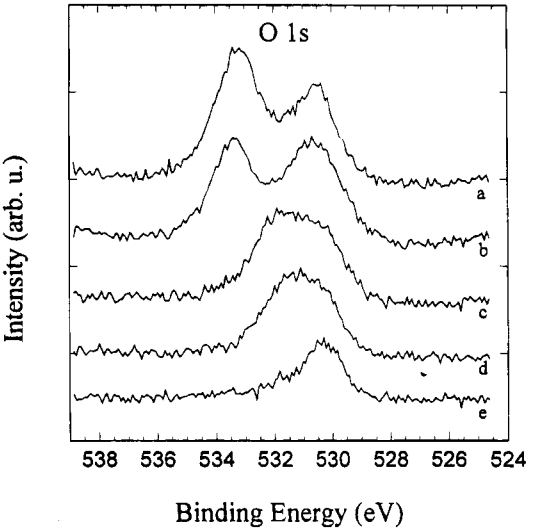

Figure 6. O 1s XPS spectra of O/Cs/graphite/Ru annealed to various temperatures. Cs and oxygen were adsorbed at 200 K with $\theta_{Cs} = 1.8$ ML and oxygen exposure of 20 L. Graphite coverage was about 0.9 ML. Annealing was done by increasing the sample temperature at a rate of 2 K/s to the specified final temperatures, and the sample was cooled down to 85 K before XPS spectra were acquired. The annealing temperatures are as follows: (a) as grown, (b) 300 K, (c) 500 K, (d) 700 K, and (e) 850 K.

2)-O on Ru, and (d) O/Cs/graphite/Ru. The O/Cs/Ru results were discussed in a recent publication.[28]

The binding energy of Cs $3d_{5/2}$ decreases slightly from 725.7 eV at sub-monolayer to 725.5 eV at the completion of the first ML, and beyond one ML, the binding energy starts to increase and reaches 726.2 eV at thick layer. For Cs adsorbed on the clean Ru(001) surface, the coverage-dependent binding energies of Cs 4d and Cs 5p core levels have been examined in detail with synchrotron-based photoemission experiments.[29,30] The coverage dependencies of Cs 3d, 4d, and 5p core levels are similar. The intensities of alkali-metal surface plasmons are sensitive to layer thickness, particularly in the thin-layer regime,[31] and we also find that no Cs surface plasmon excitation can be observed at sub-monolayer coverage.

Besides the Cs 3d core level, the spectrum of thin Cs/Ru (Figure 5a) shows unresolved bulk and surface plasmon peaks. The energy of bulk plasmon is determined to be 2.7 eV, consistent with the value given in the literature.[32] Cs 3d spectra of Cs/Ru, Cs/graphite/Ru (Figure 5b), and Cs/O/Ru (Figure 5c) are almost identical, suggesting very similar morphologies of the Cs layer in all three cases.

The fact that cesium stays on top of both (2 × 2)-O/Ru- and graphite-covered Ru surfaces has several implications. To begin with, it is noted that the Cs morphology inferred from XPS data is similar to that deduced from TDS (Figures 3 and 4). For Cs on an oxygen-covered Ru surface, the inference that Cs stays on top is permissible because of a very strong chemisorption bond between oxygen and ruthenium. However, for Cs on graphite, it is rather puzzling because the relative interaction strength is just the opposite of the Cs/O/Ru case. In contrast to the strong Ru−O interaction, the graphite layer only weakly chemisorbs on the Ru surface via Van der Waals forces. This weak interlayer interaction explains the relative ease of foreign atoms to insert themselves between layers and form a wide variety of intercalation compounds. In the present case, both TDS and XPS data indicate that the majority of Cs stays on top; as a result, no Cs graphite intercalation compound is formed.

As oxygen is adsorbed on the Cs/graphite/Ru, marked changes of Cs 3d (Figure 5d) are observed. Cs $3d_{5/2}$ peak shifts toward the lower binding energy with the peak width significantly broadened, and the plasmons are lost completely. The small peak at 730.5 eV is attributed to the satellite lines of the Mg Kα X-ray source. Meanwhile, two O 1s peaks at 533.2 and 530.4 eV binding energy are observed (Figure 6a). The oxidation of Cs has been studied extensively in both valence band and core level regions.[24,28,32−34] On the basis of these studies, the peak at 533.2 eV is attributed to cesium superoxide and the peak at 530.4 eV to cesium peroxide. In contrast, the binding energy of the O 1s peak from the (2 × 2)-O/Ru(001) overlayer is measured as 529.9 eV, in agreement with the reported value.[35] Note that the magnitude of the shift of both Cs 3d and O 1s levels, the relative ratio of oxide peaks, and the attenuation of plasmon excitation all depend on initial Cs coverage as well as oxygen coverage.

To further identify the oxygen species present on O/Cs/graphite/Ru, the surface was heated at the same rate as that employed in Figure 2 to successively higher temperatures and then quenched to 85 K before the XPS data acquisition. After annealing to 300 K, a small intensity reduction of superoxide is already noticed (Figure 6b) as compared to the unannealed case (Figure 6a). At the next higher annealing temperature of 500 K (Figure 6c), almost all superoxide has disappeared while the intensity of peroxide remains the same. The spectrum taken after annealing to 700 K (Figure 6d) is not much different from that after 500 K annealing, and both spectra exhibit a shoulder in the high binding energy side. This shoulder can be due to the O 1s core level of either CO or CO_2. Final heating to 850 K (Figure 6e) leaves a single peak, due to the peroxide species, in the spectrum. We note that the O 1s binding energy of Cs_2O is below 528 eV.[28]

Although thermal annealing causes significant changes of the O 1s spectra, the Cs 3d is little affected by it and the spectra are essentially the same as Figure 5d except that the intensities decrease due to the loss of Cs at the higher annealing temperature. The relative thermal stability of Cs oxide, Cs peroxide, and Cs superoxide grown on top of the Ru surface can be assessed by examining the enthalpies of formation of bulk oxides. The enthalpies of formation (kcal/mol, in parentheses) follow the order: Cs peroxide (−96.5) > Cs oxide (−75.9) > Cs superoxide (−63.59).[36] The observation that Cs

peroxide is the most stable species observed in the annealing experiments agrees with this trend.

For O/Cs/Ru, the same evolution, although not shown, of superoxide and peroxide peaks with respect to thermal annealing is also observed. Therefore, we can conclude that the presence of graphite does not effect the Cs−O interaction and the chemical interaction between graphite and either Cs or oxygen is very weak.

IV. Discussion

We will examine two options for the role of Cs in oxidation of graphite. The first possibility considers the formation of an intercalated surface compound; the second explores the Cs−dioxygen surface complex formation on the top of graphite overlayer.

Although alkali-intercalated graphite compounds are usually prepared by the bulk reactions in a non-UHV environment,[25,26] Lagues *et al.*[37] demonstrated that Cs-intercalated graphite could be grown in UHV by evaporating Cs onto bulk graphite. Through LEED I−V analysis, Wu and Ignatiev[38,39] found that potassium intercalated readily with graphite of higher step density (exhibiting a 6-fold symmetry LEED pattern) but not with graphite of low step density (3-fold symmetry). Using a high-resolution Auger to examine the characteristic carbon Auger peak associated with intercalated graphite, Tontegode and co-workers[40,41] concluded the cesium-intercalated graphite can be formed even on a graphite monolayer grown on either Ir, Re foils[40] or Ir, Re single crystal surfaces.[41] They also observed that a very high temperature (>2100 K) was required to completely desorb the Cs/graphite compound from Ir surfaces,[41] as compared to a temperature lower than 900 K to desorb Cs adsorbed on a metal surface.

As argued in the above section, the morphology of Cs/graphite/Ru inferred from TDS and XPS results does not support the formation of Cs-intercalated graphite in the present case. This finding is reinforced by the observation that no Cs, as probed by both TDS and XPS, remains on the surface after Cs/graphite/Ru is flashed to 1200 K. If Cs were to form an intercalated compound, Cs should be able to survive a much higher temperature[41] and could be easily detected by XPS because of the high photoemission cross section of the Cs 3d level.

On the basis of the evidence from the TDS and XPS studies, the role of Cs in the modified case becomes clear. On one hand, cesium shows little, if any, interaction with the graphite layer and does not form a Cs graphite intercalation compound. On the other hand, Cs reacts with oxygen and forms Cs peroxide and Cs superoxide. Through the oxide formation, a much greater oxygen uptake is possible as compared to the nonmodified case, for which no oxygen adsorption on the graphite surface can take place.

With more information from XPS at hand, a better understanding of O/Cs/graphite/Ru is possible, and we shall return to Figure 2 for more discussion about the TDS features. As the temperature of the O/Cs/graphite/Ru system is increased above 300 K, Cs superoxide first decomposes (Figure 6) and some oxygen is released. The liberated oxygen cannot react with graphite because a much higher reaction temperature (>700 K) is required; therefore, oxygen desorbs from the graphite-covered surface in a reaction-limited step at 380 K. This leads to an O_2 desorption peak at 380 K. As the surface temperature increases above 700 K, Cs peroxide (the only oxide species on the surface, see Figure 6) starts to decompose and freed oxygen reacts with graphite to produce CO and CO_2. This temperature range is also high enough for Cs desorption to occur. The existence of jagged peaks underneath the broad desorption envelop in CO, CO_2, and Cs TDS spectra suggests that the kinetics of the oxidation reaction are quite complex. The complexity derives from the morphology change due to Cs oxide decomposition, from diffusion of oxygen into the graphite−oxide interface, and from the desorption of oxidation products away from the interface. The existence of an inactive region where CO and CO_2 cease forming underlines the complex kinetics involved. Note that this region occurs right after very rapid CO and CO_2 formation, which suggests the inactivity is primarily due to the severe depletion of oxygen species around graphite. An induction period is therefore required for the reactants to be in close proximity so that the reaction can again proceed. Unfortunately, the complex kinetics preclude further studies with the static probes presently employed.

In summary, we made use of one aspect of Cs oxide chemistry, namely high oxygen uptake and relatively high thermal stability, to study a complete oxidation of a graphite layer. By combining TDS and XPS, Cs peroxide was found to be responsible for the enhanced oxidation and the altered reaction pathway.

Acknowledgment. This research was carried out at Brookhaven National Laboratory under Contract DE-AC02−76CH-00016 with the U.S. Department of Energy and Supported by its Division of Chemical Sciences, Office of Basic Energy Sciences.

References and Notes

(1) (a) Sjövall, P.; Kasemo, B. *Surf. Sci.* **1993**, *290*, 55. (b) Chakarov, D. V.; Sjövall, P.; Kasemo, B. *Surf. Sci.* **1993**, *287/288*, 278. (c) Sjövall, P.; Kasemo, B. *J. Chem. Phys.* **1993**, *98*, 5932. (d) Janiak, C.; Hoffmann, R.; Sjövall, P.; Kasemo, B. *Langmuir* **1993**, *9*, 3427.

(2) (a) Goodman, D. W.; White, J. M. *Surf. Sci.* **1979**, *90*, 201. (b) Goodman, D. W.; Kelley, R. D.; Madey, T. E.; Yates, J. T., Jr. *J. Catal.* **1980**, *63*, 226.

(3) Bonzel, H. P.; Krebs, H. J. *Surf. Sci.* **1980**, *91*, 499.

(4) McCarty, J. G.; Wise, H. *J. Catal.* **1979**, *57*, 406.

(5) Sau, R.; Hudson, J. B. *Surf. Sci.* **1980**, *95*, 465.

(6) Schafer, L.; Wassmuth, H.-W. *Surf. Sci.* **1989**, *208*, 55.

(7) Vink, T. J.; Bolech, M.; Gijzeman, O. L. J.; Gues, J. W. *Surf. Sci.* **1988**, *194*, 559.

(8) Labohm, F.; Engelen, C. W. R.; Gijzeman, O. L. J.; Gues, J. W.; Bootsma, G. A. *Surf. Sci.* **1983**, *126*, 429.

(9) Bonzel, H. P. *Surf. Sci. Rep.* **1987**, *8*, 43.

(10) Cotton, F. A.; Wilkinson, G. *Advanced Inorganic Chemistry*; John Wiley & Sons: New York, 1988; Chapter 4.

(11) Malik, I. J.; Hrbek, J. *J. Phys. Chem.* **1991**, *95*, 2466.

(12) Jacob, P.; Menzel, D. *Surf. Sci.* **1988**, *201*, 503.

(13) Rauscher, H; Jakob, P.; Menzel, D.; Lloyd, D. R. *Surf. Sci.* **1991**, *256*, 27.

(14) Hrbek, J. *J. Vac. Sci. Technol.* **1986**, *A4*, 86.

(15) Lauderback, L. L.; Delgass, W. N. *Surf. Sci.* **1986**, *172*, 715.

(16) Grant, J. T.; Haad, T. W. *Surf. Sci.* **1970**, *21*, 76.

(17) Wu, M.-C.; Xu, Q.; Goodman, D. W. *J. Phys. Chem.* **1994**, *98*, 5104.

(18) Castner, D. G.; Sexton, B. A.; Sormorjai, G. A. *Surf. Sci.* **1978**, *71*, 517.

(19) Rosei, R.; DeCrescenzi, M.; Sette, F.; Quaresima. C.; Savoia, A.; Perferri, P. *Phys. Rev.* **1983**, *B28*, 1161.

(20) Bezuidenhout, F.; du Plessis, J.; Viljoen, P. E. *Surf. Sci.* **1986**, *171*, 392.

(21) Land, T. A.; Michely, T.; Behm, R. J.; Hemminger, J. C.; Comsa, G. *J. Chem. Phys.* **1992**, *97*, 6774.

(22) Hrbek, J. *Surf. Sci.* **1985**, *164*, 139.

(23) Shincho, E.; Egawa, C.; Naito, S.; Tamaru, K. *Surf. Sci.* **1985**, *149*, 1.

(24) Su, C. Y.; Lindau, I.; Chye, P. W.; Oh, S.-J.; Spicer, W. E. *J. Electron Spectrosc. Relat. Phenom.* **1983**, *31*, 221.

(25) Dresselhaus, M. S.; Dresselhaus, G. *Adv. Phys.* **1981**, *30*, 139.

(26) *Chemical Physics of Intercalation*; Legrand, A. P., Flandrois. S., Eds.; NATO ASI Series, Series B; Plenum: New York, 1987; Vol. 172.
(27) (a) Kiskinova, M.; Rangelov, G.; Surnev, L. *Surf. Sci.* **1986**, *172*, 57. (b) Surnev, L.; Rangelov, G.; Kiskinova, M. *Surf. Sci.* **1987**, *179*, 283.
(28) Hrbek, J.; Yang, Y. W.; Rodriguez, J. A. *Surf. Sci.* **1993**, *296*, 164.
(29) Sham, T. K.; Shek, M.-L.; Hrbek, J. *Surf. Sci. Lett.* **1991**, *L16*, 1991.
(30) Sham, T. K.; Hrbek, J. *J. Chem. Phys.* **1988**, *89*, 1188.
(31) Tsuei, K.-D.; Heskett, D.; Baddorf, A. P.; Plummer, E. W. *J. Vac. Sci. Technol.* **1991**, *A9*, 1761.
(32) Shi. H.; Jakobi, K. *Surf. Sci.* **1992**, *276*, 12.
(33) Woratschek, B.; Sesselmann, W.; Kuppers, J.; Ertl, G.; Haberland, H. *J. Chem. Phys.* **1987**, *86*, 2411.
(34) Jupille, J.; Dolle, P.; Besancon, M. *Surf. Sci.* **1992**, *260*, 271.
(35) Fuggle, J. C.; Madey, T. E.; Steinkilberg, M.; Menzel, D. *Surf. Sci.* **1975**, *52*, 521.
(36) *Handbook of Chemistry and Physics*, 65th ed.; CRC Press: Boca Raton, FL, **1984**; p D-33.
(37) Lagues, M.; Marchand, D.; Fretigny, C.; Legrand, A. P. *Solid State Commun.* **1984**, 49, 739.
(38) Wu, N. J.; Ignatiev, A. *Phys. Rev.* **1983**, B*28*, 7288.
(39) Wu, N. J.; Ignatiev, A. *Surf. Sci.* **1989**, *218*, 283.
(40) Kholin, N. A.; Rut'kov, E. V.; Tontogode, A. Y. *Surf. Sci.* **1984**, *139*, 155.
(41) Gall, N. R.; Mikhailov, S. N.; Rut'kov, E. V.; Tontogode, A. Ya. *Surf. Sci.* **1990**, *226*, 381.

JP941573Z